

Fluorescence spectrum of heavily doped cadmium sulphide†

S. M. Girvin*

Joseph Henry Research Laboratories, Princeton University, Princeton, New Jersey 08540

(Received 14 June 1977)

The upper threshold of the fluorescence spectrum of heavily doped CdS:Cl is calculated within the framework of a simple model which is valid in the metallic regime. When various Coulomb corrections and phonon effects are taken into account, the predicted threshold location is in excellent agreement with experiment.

I. INTRODUCTION

An important testing ground for theoretical predictions about the interacting electron gas has been the study of optical-absorption spectra of heavily doped semiconductors. Because of the typically large dielectric constants and small effective masses, rather large effective densities can be obtained, allowing the Coulomb energy to be treated as a perturbation on the kinetic energy of degeneracy. Various methods of calculating the corrections to the chemical potential due to the electron-electron and electron-impurity interactions have met with success in predicting the optical-absorption threshold at very high effective densities in nonpolar semiconductors.¹⁻³

An additional source of data which has not been previously utilized is the fluorescence spectra of heavily doped semiconductors. We present here a calculation of the fluorescence threshold at various doping densities for CdS:Cl. A very simple model is used to treat the electron-impurity interaction at moderate densities where the usual expansions in the density parameter cannot be expected to work well. In addition, the effects of the electron-phonon interaction are included since CdS is a polar material. The results of the calculation are in excellent agreement with experiment.

One of the reasons why it is of interest to study the fluorescence spectrum as a function of doping is because at some critical point the density of electrons becomes high enough that a degenerate electron gas is formed. Various transport measurements have been made on CdS:Cl to study this insulator to metal transition. A correlation of changes in the fluorescence spectrum with changes in the electron transport properties can lead to a better understanding of this process. The present work complements experimental and theoretical studies which have already been made on CdS:Cl at densities below the critical density.^{4,5}

Fluorescence spectra⁶ of CdS:Cl for several different doping densities are shown in Fig. 1. As can be seen, each spectrum exhibits a well-defined threshold which increases in energy with increasing density. There are two points to which any theoretical model must address itself if it is to successfully explain this rising threshold as a simple Burstein shift.⁷ Unlike the absorption case, the wave-vector conservation rule must be violated since the photons at the threshold energy are presumed to result from the annihilation of an electron at the Fermi surface with a thermalized valence hole (which has negligible wave vector at helium temperatures). Secondly, a simple calculation of the size of the Burstein shift based on the free-electron Fermi level for a density corresponding to sample 4 gives a shift of nearly 100 meV. As can be seen in Fig. 1, the threshold for sample *L* is at, or slightly below, the band gap. This discrepancy and the violation of the $\Delta k = 0$ selection rule both occur because of the Coulomb interactions in the system.

The strength of the Coulomb interactions is determined by a dimensionless measure of the density, r_s , which is defined by

$$r_s = \left[\left(\frac{4}{3} \pi \right) n a_0^3 \right]^{-1/3}, \quad (1)$$

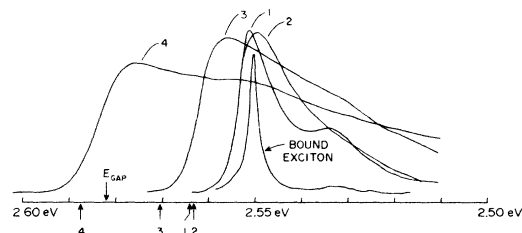


FIG. 1. Fluorescence spectra for four different CdS:Cl samples together with the predicted threshold locations for each. The doping densities for samples 1-4 are 1.5×10^{18} , 2.3×10^{18} , 6.5×10^{18} , and 12.0×10^{18} cm^{-3} , respectively.

where n is the impurity-electron density and a_0 is the effective Bohr radius. The values of r_s for all the samples are smaller (implying greater density) than that for sodium which must surely lead to a metallic state for the conduction band. This has been confirmed by three separate types of experiments: electrical conductivity,⁸ NMR Knight shift,⁹ and spin-flip Raman scattering,¹⁰ all of which indicate that CdS:Cl is fully metallic at and above a doping density of approximately $2 \times 10^{18} \text{ cm}^{-3}$.

With this metallic band picture in mind we will calculate the fluorescence-spectrum threshold presuming that it arises from the annihilation of a thermalized valence hole with a Fermi-surface electron and then show how this violation of the wave-vector conservation rule is allowed.

II. CALCULATION OF THE THRESHOLD

The upper threshold of the fluorescence spectrum is determined by the difference in energy between the ground state of the system (with N conduction electrons and no valence hole) and the lowest energy state having one valence hole and $N+1$ conduction electrons. The energy difference between these two states is determined by the Fermi level in the electron gas and the energies associated with the polarization of the lattice and the electron gas by the valence hole. In order to calculate the energies of these states one must consider all the sources of electric potential which can perturb the electron and hole energy levels. These include (i) phonons, (ii) periodic crystal potential, (iii) electron-electron interaction, (iv) electron-hole interaction, and (v) random chlorine impurity potential. The first two terms are present in both the bare and doped crystals while the last three are additional terms associated with the doping. One important effect of the doping is that dielectric screening renormalizes the contributions of the first two terms. We now consider each of these effects in detail. Numerical results for calculations presented in this section will be discussed in Sec. II A.

A. Phonons

Because of the large average interelectron distance relative to the CdS lattice constant, dielectric screening by the electron gas affects only the macroscopic longitudinal electric fields associated with lattice distortions. Since CdS is a II-VI compound, it is relatively polar and electrons and holes can couple to the longitudinal-optical (LO) phonon and to the acoustic modes. It turns out that the acoustical modes affect the electron energy by a negligible amount¹¹ (a fraction of 1 meV). We will therefore concentrate on the LO mode and

make the usual approximation that its frequency, ω_L is independent of wave vector. This is reasonable since we are concerned with only small wave vectors. (The Fermi sphere fills only a tiny fraction of the first Brillouin zone of the CdS lattice.)

The electron-phonon coupling is given by

$$V = \sum_{\mathbf{k}, \mathbf{q}} \left[\frac{4\pi e^2}{\Omega q^2} \frac{\hbar \omega_L}{2} \left(\frac{1}{\epsilon_\infty} - \frac{1}{\epsilon_0} \right) \right]^{1/2} C_{\mathbf{k}+\mathbf{q}}^\dagger C_{\mathbf{k}} (B_{-\mathbf{q}}^\dagger + B_{\mathbf{q}}), \quad (2)$$

where ϵ_∞ and ϵ_0 are the high- and low-frequency dielectric constants, Ω is the volume of the sample, $C_{\mathbf{k}}^\dagger$ is the electron creation operator, and $B_{\mathbf{q}}^\dagger$ is the phonon creation operator. This coupling leads to a correction to the conduction-band energy ΔE given by the well-known formula¹²

$$\Delta E = -\alpha \hbar \omega_L, \quad (3)$$

and a shift in the observed effective mass given by

$$m = m^* \left(1 - \frac{1}{6} \alpha \right), \quad (4)$$

where α is the polaron coupling constant, m^* is the observed mass, and m is the bare conduction-band mass.

There are similar corrections for the valence band, however, the results are modified by the anisotropy of the valence-band mass

$$\Delta E = \alpha_\perp \hbar \omega_L \arcsin(1-R)^{1/2}/(1-R)^{1/2}, \quad (5)$$

where the new coupling constant α_\perp is defined by

$$\alpha_\perp \equiv (M_\perp/m)^{1/2} \alpha, \quad (6)$$

and $R \equiv M_\perp/M_\parallel$. M_\perp and M_\parallel are, respectively, the bare valence-band masses perpendicular and parallel to the c axis of the crystal, and m is the (isotropic) bare mass of the conduction band. It turns out that the final results are not very sensitive to the hole mass and so it is convenient to only approximately evaluate the relation between the bare and dressed anisotropic masses by assuming that, in analogy with (4), the hole masses scale together

$$M_\parallel = M_\parallel^* \left(1 - \frac{1}{6} \alpha_\perp \right) \quad (7)$$

and

$$M_\perp = M_\perp^* \left(1 - \frac{1}{6} \alpha_\perp \right). \quad (8)$$

There are additional difficulties in other II-VI compounds due to phonon mixing of the closely spaced (or degenerate) valence subbands.¹³ The low symmetry of CdS lifts this degeneracy so that three sub-bands are well separated¹⁴ and it appears that one can safely ignore the presence of the lower two bands.

With the above results the bare parameters of the system may be evaluated from the experimentally measured parameters. It is now necessary

TABLE I. Electron-gas parameters based on the observed conduction-band mass (and the high-frequency dielectric constant). Energies are in meV, and $\epsilon_0 = 8.58$, $\epsilon_\infty = 5.26$, $\hbar\omega_{LO} = 36.8$, $m^* = 0.2$, and $E_B^* = 98.3$.

Sample	$k_F a_0$	r_s	ϵ_F	$\hbar\Omega_{PL}$
1	0.494	3.88	24.0	44.5
2	0.571	3.36	32.1	55.3
3	0.803	2.39	63.4	92.2
4	0.990	1.94	96.4	126.2

to evaluate the polaron effects in the presence of dielectric screening by the electron gas.¹⁵ The reason that this screening is important can be seen from the numbers in Table I. For the highest-density sample the electron plasma frequency Ω_{PL} is approximately three times larger than the LO-phonon frequency. This means that the electron gas has time to respond to and partially cancel out the relatively slowly varying electric field associated with the lattice vibration. This results in a reduction of the electron-phonon coupling and a lowering of the frequency of the phonon mode. The

energy associated with the long-range electric field of the LO-mode breaks the degeneracy of the LO and TO frequencies. If this electric field were completely screened out the LO frequency would drop from ω_L to ω_T , the TO frequency. We make the simplifying assumptions (valid in the high-density limit) that the renormalized LO frequency is equal to ω_T and that the reduction in the electron-phonon coupling can be represented by static Thomas-Fermi screening. These should be good approximations, at least for sample L, where $\Omega_{PL} \sim 4\omega_T$.

As a result of screening and the approximate particle-hole symmetry¹⁶ above and below the Fermi surface, the screened polaron contribution to the electron chemical potential is quite small (~ 1 meV) and will be neglected. This is not the case for the valence-band hole since it is distinguishable from the conduction electrons (and thus not subject to exclusion effects) and is more strongly coupled to the phonons (due to its heavier mass). Within the approximations that have been made, the lowest-order energy shift for the hole is given by

$$\Delta E = -\left(\frac{\omega_L}{\omega_T}\right)^{1/2} \frac{\alpha_\perp \omega_L}{2} \left\{ \frac{-K}{(1-K^2)(1+K\sqrt{R})} - \frac{2(K^2-2)}{(1-R)^{1/2}(1-K^2)^{3/2}} \arctan \left[\left(\frac{1-K}{1+K}\right)^{1/2} \left(\frac{1-\sqrt{R}}{1+\sqrt{R}}\right) \right] \right\} \quad (9)$$

for $K < 1$, and

$$\Delta E = -\left(\frac{\omega_L}{\omega_T}\right)^{1/2} \frac{\alpha_\perp \omega_L}{2} \left[\frac{-K}{(1-K^2)(1+K\sqrt{R})} - \frac{K^2-2}{(1-R)^{1/2}(K^2-1)^{3/2}} \ln \left| \frac{1 + [(K-1)/(K+1)]^{1/2} [(1-\sqrt{R})/(1+\sqrt{R})]^{1/2}}{1 - [(K-1)/(K+1)]^{1/2} [(1-\sqrt{R})/(1+\sqrt{R})]^{1/2}} \right| \right] \quad (10)$$

for $K > 1$. The parameter K is defined by

$$K \equiv (m/M_\perp)^{1/2} q_{TF} R_p^*, \quad (11)$$

where q_{TF} is the Thomas-Fermi wave vector and R_p^* is the screened polaron radius given by

$$R_p^* = a_0 |E_B / \hbar\omega_T|^{1/2}, \quad (12)$$

where E_B is the effective Rydberg (based on the bare conduction-band mass).

The screened polaron correction to the effective mass turns out to be quite small in both bands and will be neglected.

This completes the analysis necessary to establish the shift in the fluorescence threshold due to phonon effects.

B. Periodic crystal potential

Doping induces two changes in the periodic crystal potential which must be investigated. First we consider the short-range difference in core poten-

tial between sulphur and the substituted chlorine (the long-range Coulomb part of the Cl potential will be treated later). The magnitude of the effect on the band gap may be estimated by assuming that the difference in potential between the two species is of the same order of magnitude as the difference between sulphur and selenium. The semiconductor cadmium selenide has a band gap approximately 0.7 eV smaller than that of CdS. Assuming that the band-gap shift in CdS:Cl is proportional to the relative Cl impurity density (6×10^{-4} at the highest doping level), one obtains a shift of less than 0.5 meV in the worst case. This is negligible on the scale of expected uncertainty in the present calculation.

The second factor that must be considered is the screening of the periodic crystal potential by the electron gas. One expects this to be a small effect since the length scale of the periodic potential is much smaller than the screening length.

Unfortunately, a simple Thomas-Fermi estimate of the screening is not valid at the large wave vectors associated with the crystal potential necessitating a different approach to the problem. This was achieved by estimating the change in energy of the electron gas due to the spatial modulation of the electronic wave functions by the crystal potential. This energy was estimated to be less than 1 meV and so will be neglected.

In summary, it appears that one can safely assume that the CdS band structure is unaffected by the doping.

C. Electron-electron interaction

Theoretical studies of the interacting electron gas invariably assume that the electrons are imbedded in a uniform positive background whose only purpose (and whose only effect) is to provide overall charge neutrality. The Fermi level of such a system can be calculated with fair accuracy, at least in the high density limit. Of course CdS:Cl does not present such a simple background for the electrons. In order to make contact with the standard calculations it is necessary to assume that the effect on the electrons of the nonuniform background may be represented by a constant energy shift and an effective mass correction. This approach works well in the alkali metals¹⁷ where the background is nonuniform (although it does have high translational symmetry).

Using the correlation energy expression of Nozières and Pines¹⁸ one obtains the following result for the Fermi level, ϵ_F in terms of the Fermi wave vector, k_F :

$$\epsilon_F = \left\{ (k_F a_0)^2 - (2/\pi)(k_F a_0) - 0.031 \ln [\alpha (k_F a_0)] - 0.125 \right\} E_B, \quad (13)$$

where $\alpha \equiv (4/9\pi)^{1/3}$. The first and second terms are, respectively, the kinetic energy of degeneracy and the exchange energy. The remaining terms represent the correlation energy.

This establishes the energy shift of an electron on the Fermi surface due to its interaction with the other electrons. We now turn to a calculation of the energy shift of a hole at the top of the valence band due to its interaction with the electrons.

D. Electron-hole interaction

We are considering only a single valence hole and it is distinguishable from particles in the conduction band (because it has a different band index) so that, unlike the electron case, there is no kinetic energy of degeneracy and no exchange energy. This leaves only the correlation energy which we now calculate. The correlation energy arises

from the polarization of the electron gas by the valence hole and is given in lowest order by

$$\Delta E = -\frac{\hbar}{\pi(2\pi)^3} \int d^3 q \int_0^\infty d\beta \frac{4\pi e^2}{\epsilon_\infty q^2} \times \text{Im} \left(\frac{-1}{\epsilon(q, \beta)} \right) \frac{1}{T(\vec{q}) + \hbar\beta}, \quad (14)$$

where $T(\vec{q})$ is the kinetic energy in the (anisotropic) valence band, and $\epsilon(q, \beta)$ is the dielectric function for the electron gas. Equation (14) was evaluated numerically in the following manner. There are two contributions¹⁴ to the imaginary part of the inverse dielectric function, one from the plasmon pole and one from the branch cut due to single-particle excitations. The contribution due to the singularity at the plasmon pole was obtained from the numerical evaluation of the fraction of the f sum rule¹⁹ exhausted by the single particle branch cut, thus avoiding the difficulty of handling the plasmon singularity numerically. The self-energy contributions from the plasmon and single-particle excitation were approximately equal causing the relaxation energy to be considerably larger than that obtained by simpler approximations for the dielectric function.²⁰

This establishes the correction to the fluorescence threshold due to the polarization of the electron gas by the valence hole.

E. Random chlorine potential

The electronic configuration of an ionized chlorine donor is the same as that of the sulphur it replaces. This plus the small size of the electronic core relative to the effective Bohr radius in the solid causes the Cl impurity to appear hydrogenic against the CdS background. This picture is confirmed by the fact that the donor binding energy²¹ (33 meV) is very close to the Rydberg ($e^2/2a_0\epsilon_0 = 37$ meV). In order to be able to make an estimate of the energy shift and effective mass at the Fermi level due to this potential, the Cl atoms will be assumed to be distributed on a periodic superlattice within the CdS lattice. The perturbation whose effect we now investigate is the difference in potential between this superlattice of positive point charges and the uniform positive background which was assumed in the previous sections.

With the assumptions that have been made, the Cl superlattice system is equivalent, except for scale factors, to the metallic hydrogen system first studied by Wigner and Huntington.²² Using the Wigner-Seitz method, they calculated the location of the conduction-band bottom E_H , and the effective mass. The correction to the CdS conduc-

tion-band bottom is the difference between E_H and the band bottom, E_0 for a uniform positive background. For a uniform positive charge in the Wigner-Seitz cell, the electronic wave function at the band bottom is essentially flat so that E_0 is simply the average potential in the cell due to the background, and is given by

$$E_0 = -2.4 E_B / r_s, \quad (15)$$

where all the parameters are based on the low-frequency dielectric constant ϵ_0 .

In addition to a rigid band shift of $E_H - E_0$, there is also an effective-mass correction to the Fermi level. The Wigner-Huntington calculation shows that the effective mass differs from unity by only a few percent in the range of relevant densities. This is important on the scale of interest in metallic hydrogen but is negligible in the present problem (there are presumably bigger errors associated with the neglect of the random nature of the potential). The Wigner-Huntington effective mass was calculated by a perturbation technique²³ which works well for the alkali metals (including lithium which has $m^*/m = 1.6$) and so seems reliable. It seems at first a little surprising that the metallic hydrogen effective mass is not large since the mass in the alkali series increases with decreasing atomic number. Wigner and Huntington point out that the core potential is strong and that the wave function at the bottom of the band is severely distorted as might be expected. However, because of the wide separation of the hydrogenic energy levels, this distortion does not change with momentum as it does in lithium and so the mass is not severely affected. This can be confirmed experimentally for the case of heavily doped CdS:Ga. The plasma frequency based on the bare conduction-band mass produces a predicted infrared reflectivity which is consistent with the data.²⁴

The energy of the valence-band hole is also affected by the impurity potential. The change in potential from that of a uniform positive background to a hydrogenic potential is screened by the electron gas. This screening was not considered in the Wigner-Seitz calculation of the electron energy shift because, to a good approximation, electron-electron correlations allow only one electron at a time in the Wigner-Seitz cell.²⁵ The energy shift at the top of the valence band given by lowest-order perturbation theory is

$$\Delta E = \frac{-3e^2}{\epsilon_0 a_0 r_s y^2} (1+y) e^{-y} \left(1 - \frac{3(y \cosh y - \sinh y)}{y^3} \right), \quad (16)$$

where $y \equiv q_{TF} a_0 / r_s$.

This completes the analysis necessary to estab-

lish the net energy shift of a Fermi level conduction electron relative to a hole at the top of the valence band due to the chlorine impurity potential.

III. NUMERICAL RESULTS

This section will outline the numerical results for the calculations presented in the previous sections. The first step is to take out the polaron effects in order to find the bare parameters of the conduction band. Using as input information: (a) dielectric constants²⁶: $\epsilon_0 = 8.58$, $\epsilon_\infty = 5.26$; (b) observed mass¹⁴: $m^* = 0.20$; (c) LO phonon energy²⁶: $\hbar\omega_{LO} = 36.8$ meV; one obtains: (d) polaron coupling constant: $\alpha = 0.60$; (e) bare mass: $m = 0.18$; (f) bare Rydberg: $E_B^0 = 33.3$ meV, $E_B^\infty = 88.5$ meV; (g) polaron energy: $\Delta E = \alpha \hbar\omega_{LO} = 22$ meV. The effective density and related quantities based on these bare parameters are shown in Table II.

The next step is to find the bare parameters of the valence band. Using the observed masses¹⁴: $M_\uparrow^* = 0.7$ and $M_\downarrow^* \sim 5$, one obtains: (a) polaron coupling constant: $\alpha_\perp = 1.07$; (b) bare masses: $M_\perp = 0.57$, $M_\parallel = 2.7$; (c) polaron energy: $\Delta E = 49$ meV. The heavy-hole mass M_\parallel is not very well known,¹⁴ however the hole-relaxation energy was found to depend only weakly on this quantity.

Once the bare parameters of the system have been established, one may calculate the various relevant energies discussed in the previous sections: (a) The Fermi energy of the interacting electron gas with a uniform positive background. (b) The difference in conduction band bottom between a uniform positive background and the metallic hydrogen potential. (c) The difference in valence band top between a uniform positive background and the metallic hydrogen potential. (d) The shift in band gap due to the polarization of the electron gas by the hole. (e) The shift in the band gap due to the energy difference between the screened and unscreened polaron in each band.

The full set of numbers is displayed in Table III. The final predictions for the threshold locations are marked on the data displayed in Fig. 1. The agreement is excellent on the scale of the various

TABLE II. Electron-gas parameters based on the bare conduction-band mass (and the high-frequency dielectric constant). Energies are in meV, and $\epsilon_0 = 8.58$, $\epsilon_\infty = 5.26$, $\hbar\omega_{LO} = 36.8$, $m = 0.18$, and $E_B = 88.5$.

Sample	$k_F a_0$	r_s	ϵ_F	$\hbar\Omega_{PL}$
1	0.549	3.50	29.6	52.1
2	0.634	3.03	39.6	64.7
3	0.892	2.15	78.3	108.0
4	1.10	1.74	119.0	147.8

TABLE III. Energies (in meV) relevant to the calculation of the spectrum threshold. (A) Fermi energy of the interacting electron gas. (B) Band bottom in metallic hydrogen. (C) Band bottom with uniform positive background. (D) Hole impurity interaction. (E) Relaxation energy of the electron gas around the valence hole. (F) Bare conduction polaron energy. (G) Bare valence polaron energy. (H) Screened valence polaron energy. (I) Sum of all of the above, giving the threshold location relative to the undoped band gap.

Sample	A	B	C	D	E	F	G	H	I
1	-12.4	-50.9	+36.3	+1.7	-36.1	+22.1	+48.8	-27.1	-17.7
2	-8.8	-57.9	+42.2	+2.2	-41.0	+22.1	+48.8	-26.3	-18.6
3	+9.4	-77.5	+59.1	+3.7	-53.1	+22.1	+48.8	-23.8	-11.3
4	+32.9	-93.8	+73.2	+5.0	-61.32	+22.1	+48.8	-23.3	+5.3

energies involved ($\hbar^2 k_F^2/2m \sim 100$ meV for sample 4). Recall that the approximations which have been made are accurate only in the high-density limit where the plasma frequency is much larger than the phonon frequency. This condition is fairly well satisfied for sample 4 ($\Omega_{PL}/\omega_{LO} = 3.4$) but is not well satisfied for the less dense samples. The assumption that the phonons are statically screened by the electron gas underestimates the phonon coupling at lower densities thereby raising the predicted threshold somewhat. This is believed to account for the small systematic discrepancies between the predicted and observed thresholds for the lower-density samples.

IV. WAVE-VECTOR NONCONSERVATION

The fluorescence spectrum exhibits a well-defined upper threshold whose location is accurately predicted by the present model. Recall however that implicit in the calculation of the threshold location was the assumption that the momentum distribution of the valence hole overlapped that of the Fermi-surface electrons (in order for the annihilation of a Fermi surface electron to be optically allowed). The validity of this assumption must now be investigated.

The momentum conservation which is the source of the $\Delta k = 0$ rule is a consequence of the translational symmetry of the crystal. The random impurity distribution breaks this symmetry and allows a violation of the $\Delta k = 0$ rule. The momentum distribution of the valence hole is strongly affected by impurity scattering because the hole is relatively heavy and not subject to exclusion principle constraints. A simple first-order perturbation estimate of the radial momentum distribution for the lowest-energy hole state yields

$$\rho(q) d\left(\frac{q}{k_F}\right) = 8 \left(\frac{N}{\Omega k_F^3} \right) \left[\frac{e^2 k_F}{\epsilon_F} \left(\frac{M}{m} \right) \frac{k_F/q}{1 + q_{TF}^2/k_F^2} \right]^2 d\left(\frac{q}{k_F}\right), \quad (17)$$

where N/Ω is the impurity density and M/m is the ratio of valence- to conduction-band mass. The

overall strength and width of the momentum distribution given by (17) is such that the $\Delta k = 0$ rule must completely break down. This is easily seen experimentally in the absorption spectrum of doped germanium. The strength of the indirect absorption threshold (which requires a very large momentum transfer relative to the $\hbar k_F$ in the present problem) is known to rise rapidly with impurity density.²⁷

V. FLUORESCENCE SPECTRUM BELOW THE CRITICAL DENSITY

As was mentioned earlier, the present work complements experimental⁴ and theoretical⁵ work on the fluorescence spectrum of CdS:Cl at densities below the critical density for the metal-insulator transition. The theory of Hanamura⁵ notes that the fluorescence spectrum appears to grow continuously out of the bound exciton line and attempts to explain this in terms of a random stark shifting of the bound exciton line by impurity electric fields. The slow increase in the fluorescence threshold with doping density is explained as a decrease in the exciton binding energy due to this stark shifting. The predicted spectral shape (using one adjustable parameter) agrees fairly well with the data. Because of the rather slow rise in threshold with density agreement can be obtained at densities as high as $4.4 \times 10^{18} \text{ cm}^{-3}$ which is well into the metallic regime. The present theory, which assumes a metallic state, accounts for the rather slow rise in the threshold as a function of doping in terms of corrections to the chemical potential due to the Coulomb and lattice interactions.

VI. SUMMARY

The fluorescence spectrum of heavily doped CdS:Cl exhibits a well-defined upper threshold whose location is accurately predicted by a model which relates the threshold to the Fermi level of the impurity electron gas and the self-energy of the valence band hole. The calculation takes into account phonon effects and treats the random impurity potential by the Wigner-Seitz method.

ACKNOWLEDGMENTS

The author is grateful to J. J. Hopfield for the original suggestion of this problem and the sub-

sequent guidance which he provided. The support of Indiana University during the completion of this manuscript is also gratefully acknowledged.

†Research supported in part by the NSF.

*Present address: Physics Dept., Indiana University, Bloomington, Ind. 47401.

¹P. A. Wolff, Phys. Rev. 126, 405 (1962).

²V. L. Bonch Bruevich, *The Electronic Theory of Heavily Doped Semiconductors* (Elsevier, New York, 1966).

³Peter R. Rimbey and G. D. Mahan, Phys. Rev. B 10, 3419 (1974).

⁴Hiroshi Kukimoto, Shigeo Shionoya, Seizo Toyotomi, and Kazuo Morigaki, J. Phys. Soc. Jpn. 28, 110 (1970).

⁵Eiichi Hanamura, J. Phys. Soc. Jpn. 28, 120 (1970).

⁶These spectra were kindly made available to the author by Dr. S. Geschwind of Bell Laboratories.

⁷E. Burstein, Phys. Rev. 93, 632 (1954).

⁸S. Toyotami and K. Morigaki, J. Phys. Soc. Jpn. 25, 807 (1968).

⁹F. D. Adams, D. R. Locker, D. C. Look, and L. Carlton-Brown, Phys. Rev. B 4, 2115 (1971).

¹⁰S. Geschwind, R. Romestain, and G. E. Devlin, J. Phys. (Paris) C 4, 313 (1976).

¹¹G. D. Mahan and J. J. Hopfield, Phys. Rev. Lett. 12, 241 (1964).

¹²J. M. Ziman, *Elements of Advanced Quantum Theory* (Cambridge U.P., London, 1969), p. 47.

¹³G. Beni and T. M. Rice, Phys. Rev. B 15, 840 (1977).

¹⁴D. G. Thomas and J. J. Hopfield, Phys. Rev. 116, 573

(1959).

¹⁵The development in this section is based on that of G. D. Mahan, in *Polarons in Ionic Crystals and Polar Semiconductors*, edited by Jozef T. Devreese (North-Holland and American Elsevier, New York, 1971), p. 533.

¹⁶S. Engelsberg and J. R. Schrieffer, Phys. Rev. 131, 993 (1963).

¹⁷Frederick Seitz, *The Modern Theory of Solids* (McGraw-Hill, New York, 1940), p. 345.

¹⁸P. Nozières and D. Pines, Phys. Rev. 111, 442 (1958).

¹⁹D. Pines, *Elementary Excitations in Solids* (Benjamin, New York, 1964), p. 134.

²⁰G. D. Mahan, Phys. Rev. 153, 882 (1967).

²¹C. H. Henry and K. Nassau, Phys. Rev. B 2, 997 (1970).

²²E. P. Wigner and H. B. Huntington, J. Chem. Phys. 3, 764 (1935).

²³Frederick Seitz, Ref. 17, p. 354.

²⁴R. J. Bell, Phys. Lett. A 24, 576 (1967).

²⁵Frederick Seitz, Ref. 17, p. 355.

²⁶D. L. Rode, *Semiconductors and Semimetals* (Academic, New York, 1975), Vol. 10, p. 84.

²⁷J. I. Pankove and P. Aigrain, Phys. Rev. 126, 956 (1962).